Understanding millimetre wave FMCW radars

Article · January 2005

CITATIONS
162

READS
9,042

1 author:

Graham Brooker
The University of Sydney
103 PUBLICATIONS **1,248** CITATIONS

SEE PROFILE

1st International Conference on Sensing Technology
November 21-23, 2005 Palmerston North, New Zealand

Understanding Millimetre Wave FMCW Radars

Graham M Brooker
Australian Centre for Field Robotics, University of Sydney, Sydney, Australia
gbrooker@acfr.usyd.edu.au

Abstract

This paper discusses the design and implementation of millimetre wave FMCW radar systems. It examines the homodyne process before examining issues of chirp linearity and range resolution. It concludes with an overview of the effects of oscillator phase noise and reflected power on the performance of these systems.

Keywords: frequency modulated continuous wave, radar, millimetre wave, range resolution, phase noise

1 Introduction

Frequency Modulated Continuous Wave (FMCW) radars operate using the homodyne principle, i.e., a CW radar in which the oscillator serves as both the transmitter and local oscillator [1] p16-3 . In the millimetre wave band, varactor tuned Gunn oscillators are often used to generate the chirp [2]. In Figure 1, the CW signal is modulated in frequency to produce a linear chirp which is radiated toward a target through an antenna. The echo received T_p seconds later is mixed with a portion of the transmitted signal to produce a beat signal at a frequency f_b. which is proportional to the round-trip time T_p.

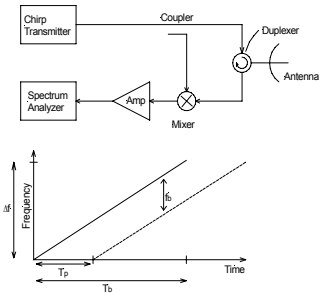

Figure 1: The FMCW concept

2 Determining the Beat Frequency

For an analytical explanation, the change in frequency, ω_b, with time can be described by

$$\omega_b = A_b t \,. \tag{1}$$

Substituting into the standard equation for FM and simplifying, we obtain

$$v_{fm}(t) = A_c \cos\left[\omega_c t + \frac{A_b}{2} t^2\right]. \tag{2}$$

A portion of the transmitted signal is mixed with the returned echo by which time the transmit signal frequency will be shifted from that of the received signal because of the round trip time T_p.

$$v_{fm}(t-T_p) = A_c \cos\left[\omega_c (t-T_p) + \frac{A_b}{2}(t-T_p)^2\right] \tag{3}$$

Calculating the product of (2) and (3) and expanding

$$v_{out}(t) = \frac{A_c^2}{2}\left[\begin{array}{l}\cos\left\{\left(2\omega_c - A_b T_p\right)t + A_b t^2 + \left(\frac{A_b}{2}{T_p}^2 - \omega_c T_p\right)\right\} \\ + \cos\left\{A_b T_p . t + \left(\omega_c T_p - \frac{A_b}{2}{T_p}^2\right)\right\}\end{array}\right] \tag{4}$$

The first cosine term describes a linearly increasing FM signal (chirp) at about twice the carrier frequency with a phase shift that is proportional to the delay time T_p. This term is generally filtered out either actively, or more usually in radar systems because it is beyond the cut-off frequency of the mixer and subsequent receiver components. The second cosine term describes a beat signal at a fixed frequency which can be obtained by differentiating the instantaneous phase term with respect to time as shown

$$\begin{aligned} f_b &= \frac{1}{2\pi}\frac{d}{dt}\left[A_b T_p . t + \left(\omega_c T_p + \frac{A_b}{2}{T_p}^2\right)\right] \\ &= \frac{A_b}{2\pi} T_p \end{aligned} \tag{5}$$

It can be seen that the beat frequency is directly proportional to the round trip time to the target, T_p, as postulated at the start of this paper.

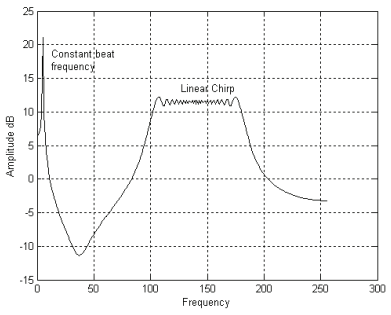

Figure 2: Spectrum FMCW receiver output

Figure 2 shows the output signal spectrum prior to filtering that contains both the linear chirp and the constant frequency components.

For a chirp duration of T_b seconds, the spectrum of the beat signal will be resolvable to an accuracy of $2/T_b$ Hz (between minima) [3] assuming that $T_b >> T_p$ as shown in Figure 3. It is common practice to define the resolution bandwidth of a signal δf_b between its 3dB (half power) points, which in this case fall within the $1/T_b$ region centred on f_b.

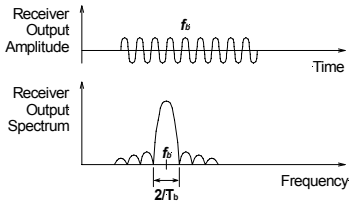

Figure 3: Output spectrum for a truncated sinusoid

The rate of change of frequency (chirp slope) in the linear case is constant and equal to the total frequency excursion Δf divided by the time T_b. The beat frequency is then given by

$$f_b = \frac{A_b}{2\pi} T_p = \frac{\Delta f}{T_b} T_p \,. \tag{6}$$

From the basics of radar, the round trip time T_p to the target and back can be written in terms of the range as

$$T_p = \frac{2R}{c} \,, \tag{7}$$

which can be substituted into (6) to give the classical FMCW formula, [4] p678, that relates the beat frequency and the target range

$$f_b = \frac{\Delta f}{T_d} \frac{2R}{c} \,. \tag{8}$$

3 Range Resolution

Extrapolating from (8) it can be seen that the range resolution, δR, can be obtained by substituting the frequency resolution δf_b, as follows

$$\begin{aligned} R &= \frac{T_d c}{2\Delta f} f_b \\ \delta R &= \frac{T_d c}{2\Delta f} \delta f_b \end{aligned} \tag{9}$$

It was shown earlier that $\delta f_b \approx 1/T_d$, which when substituted into (9) results in the well known relationship between chirp bandwidth and range resolution

$$\delta R = \frac{c}{2\Delta f} \,. \tag{10}$$

Unfortunately the range resolution is also a function of the chirp linearity. As shown conceptually in Figure 4, if the chirp is not linear, then the beat frequency for a point target will not be constant and the range resolution will suffer.

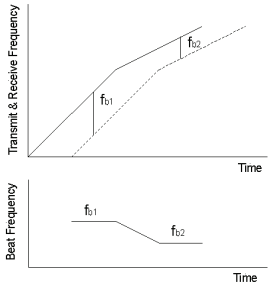

Figure 4: Effect of chirp nonlinearity on the beat frequency

It can be shown that if the nonlinearity is quadratic [5], then the range resolution degrades linearly with range

$$\delta R = R.Lin \,, \tag{11}$$

where the linearity, Lin is defined as the change in chirp slope, $S = df/dt$, normalised by the minimum slope,

$$Lin = \frac{S_{\max} - S_{\min}}{S_{\min}} \,. \tag{12}$$

This limitation is one of the fundamental problems with the FMCW system and has been addressed in a number of ways that are discussed later in this paper.

If the non-linearised case is considered, it is obvious that as the chirp bandwidth is increased the range resolution will improve, but simultaneously the total non-linearity increases and the range resolution degrades. The combined effect can be determined by

$$\delta R = \sqrt{\left(\frac{c}{2\Delta f}\right)^2 + (R.Lin)^2} \,. \tag{13}$$

A chirp bandwidth beyond that which is required to achieve the range resolution is often used as it provides additional clutter smoothing [4] p681.

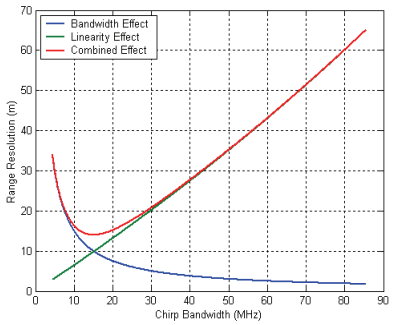

Figure 5: Effect of optimising the chirp bandwidth on the range resolution of a non linearised FMCW radar illuminating a target at 500m

For closed-loop linearisation where an almost perfectly linear chirp is generated, it is no longer practical to try to optimise the bandwidth. In this case

the resolution degrades with range in a predictable way, with the resolution determined by the chirp bandwidth at close range, and by the linearity thereafter.

3.1 Improving the Range Resolution

To improve the range resolution a number of practical methods of linearising the chirp signal have been considered. A common method uses the programmed correction stored in a lookup table which is then clocked through a digital to analog converter (DAC). The VCO temperature must either be held constant or different lookup tables must be used to accommodate variations in the oscillator characteristic.

The all-analog configuration shown in Figure 6, is an alternative. It uses an analog multiplier to produce a quadratic voltage that is added to the linear ramp to perform the correction.

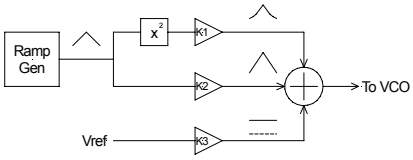

Figure 6: Quadratic frequency chirp correction circuit using an analog multiplier chip

The obvious method to determine the effectiveness of a linearisation technique is to examine the beat frequency spectrum for a point target, at a reasonable range (>500m). However, this is often not practical, and so an alternative more compact method is used.

In essence all a FMCW radar does is mix a portion of the transmitted signal with the received signal to produce a beat signal, the frequency of which is proportional to the range. As the name implies, a delay-line discriminator [6] p159 performs the same function using an electrical delay-line rather than the genuine round-trip delay to a target and back.

The most basic delay-line is a length of coaxial or fibre-optic cable, but these are usually too bulky for practical applications, so surface acoustic wave (SAW) devices are used to fulfil this function as shown in Figure 7.

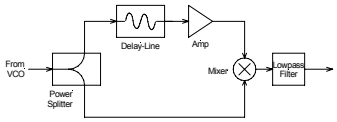

Figure 7: Delay-line discriminator

Disadvantages of SAW delay-lines are their high insertion loss (>35dB) limited bandwidth (<300MHz) and an operating frequency of less than 1GHz. For millimetre-wave radar applications, the VCO frequency must therefore be down-converted to an appropriate IF (typically 700MHz) to take advantage of commercially available delay-lines.

The spectrum of the output of the discriminator is then examined to determine the effectiveness of the linearisation process. The centre frequency defines the chirp slope, and the 3dB bandwidth, the linearity. In Figure 8, the discriminator outputs are shown for a Hughes VCO [7] both completely unlinearised and after open-loop linearisation.

Note that the width of the signal is reduced from 80kHz to 10kHz which implies an improvement in linearity from 0.26 to just over 0.03.

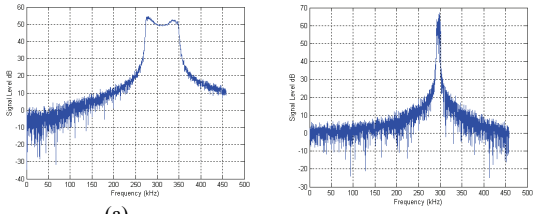

(a) (b)

Figure 8: Discriminator output spectra for (a) an unlinearised Hughes VCO and (b) after open-loop correction

Unfortunately, many of the millimetre-wave voltage controlled oscillators do not exhibit a well behaved quadratic nonlinearity characteristic and using a lookup table is the only viable linearisation technique.

The delay-line discriminator can be used as a feedback element to close the linearisation loop [8], if it is remembered that the loop must maintain a constant rate-of-change of frequency and not frequency as is more usual.

The delay-line discriminator is effectively a differentiator in the frequency domain and produces a constant output frequency if the frequency slope is constant. Thus to close the loop correctly, an integrator must be implemented in the feedback path to produce the structure shown in Figure 9.

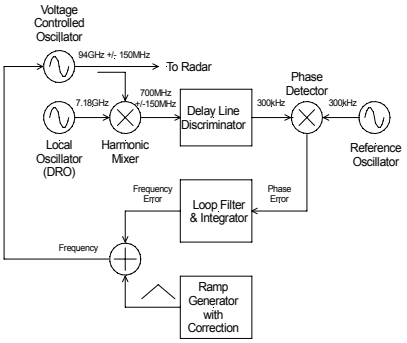

Figure 9: Schematic diagram showing the process of chirp linearisation

The implementation of a loop filter that exhibits the appropriate locking bandwidth, low phase-noise and good suppression of spurious signals requires careful design and layout. Even so, it is nearly impossible to eliminate the spurious signals from the receiver spectrum completely.

The following measured results show the output spectrum of the delay line-discriminator for both open and closed loop linearisation of a 77GHz radar from which the chirp linearity can be determined.

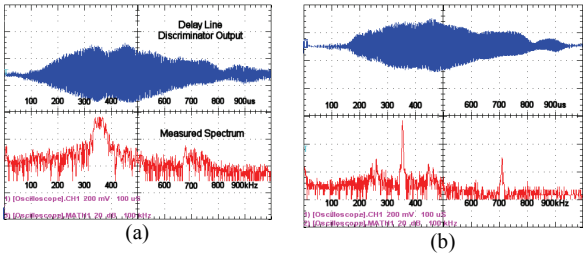

Figure 10: Measured delay line discriminator output showing (a) open loop and (b) closed loop signals

One of the issues with controlling only the chirp slope only is that the centre frequency will drift in a random fashion with time. Figure 11 shows the measured loop error voltage over 200 sweep periods.

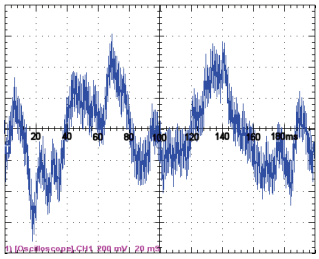

Figure 11: Measured loop error signal that shows a random variation in the VCO centre frequency

The high frequency component of the signal is the correction factor that is added to each 1ms sweep to achieve the required closed-loop linearity.

Alternatives to using temperamental millimetre wave VCO technology and the associated linearisation circuitry are to use a fractional division phase locked loop to generate the linear ramp [9], or to use direct digital synthesis (DDS) and an up-conversion stage.

4 Effects of Phase Noise

A single antenna or even a dual antenna configuration mounted behind a radome results in a significant portion of the transmitter power leaking into the receiver. This is not an issue for a pulsed radar that separates its transmit and receive functions in time, but it does pose significant problems for an FMCW system that must receive echoes while it is transmitting. These problems include a limit to the maximum transmit power and a requirement for careful matching of the antenna and circulator to minimise the magnitude of the reflections and leakage back into the receiver.

For short range operation, the FMCW radar may transmit a signal power up to a maximum of 50mW (17dBm) while simultaneously receiving signals smaller than -80dBm, a difference of about 100dB. The best low insertion loss y-junction circulators seldom offer isolations much better than 20dB, for leakage path L_1 shown in Figure 12, and the return loss of a good antenna seldom exceeds -25dB for leakage path L_2. In addition, if there is a radome, leakage path L_3 is likely to be of the same order of magnitude as L_2, so at best the leakage signal will be some 80dB higher than the received signal.

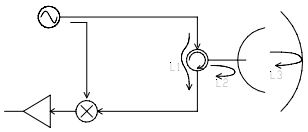

Figure 12: Oscillator signal leakage paths

Because the direct path and the leakage paths are about the same length, the frequency of the signal that reaches the mixer by the two routes will be the same, and so it will operate as a phase detector to produce an output proportional to the difference between the two path lengths. If the leakage signal is too large it can bias the mixer out of its operating region into saturation and degraded performance results [10]. This does not occur if the path lengths are matched making the difference, $\Delta R = 0$. In this case the output bias voltage is zero and the mixer performs normally for AC signals.

In addition to this desensitisation effect, which is well documented [11], the leakage signal also introduces additional noise into the receiver over and above the thermal noise level. This additional noise is due to the phase noise of the transmitter.

The phase noise produced by a number of 94GHz VCOs has been measured by us and varies between -69 and -74dBc/Hz at an offset of 100kHz. The power spectrum $S(f)$ is given by the following function for a Millitech oscillator.

$$S(f) = 10^{7.85} f^{-3.05}. \tag{14}$$

If the phase noise contributions are included in the equations derived for the FMCW beat signal, then the equations can be rewritten as

$$v_{out}(t) = \frac{A_c^2}{2}\cos\left[A_b T_p .t + \left(\omega_c T_p - \frac{A_b}{2} T_p{}^2\right) + \phi(t) - \phi(t - T_p)\right] \tag{15}$$

The transfer function that models the process of obtaining the difference frequency of which one is just a delayed version of the other is

$$H(j\omega) = 1 - e^{-j\omega T_p}, \tag{16}$$

making the magnitude squared function

$$\left|H(j\omega)\right|^2 = 2\left(1 - \cos\omega T_p\right). \tag{17}$$

The output power density spectrum for a phase noise input of $S(f)$ is the product of this transfer function and the noise power spectrum

$$S_r(f) = 2S(f)(1 - \cos 2\pi f T_p). \tag{18}$$

The noise power relative to the carrier at an offset Δf from the carrier in dB/Hz is given by

$$N(\Delta f) = 10\log_{10} 2S(\Delta f)(1-\cos 2\pi\Delta f T_p)\,. \qquad (19)$$

In the leakage case, the round-trip time is replaced by its equivalent path length difference $T_p = \Delta R/c$ and the modified phase noise spectrum plotted in Figure 13.

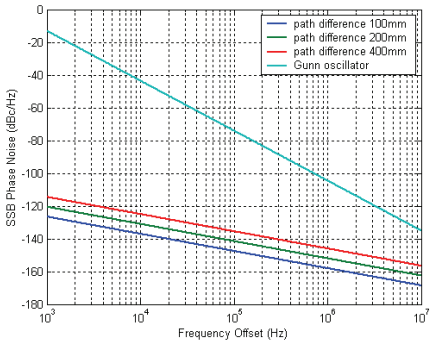

Figure 13: Gunn Oscillator phase noise levels due to leakage with path length differences as a parameter

This figure displays the phase noise as a function of frequency relative to the transmitted power level Hence if the oscillator power is P_t dBm and the leakage is L_{leak}, then the power levels must be scaled by $P_t - L_{leak}$ to obtain the actual noise power density.

To obtain the noise power level out of each range gate, the power density must be integrated over the gate bandwidth, β. For a radar with P_t = 14dBm, L_{leak} = 20dB and β = 1kHz, the noise power levels must be increased by 14 – 20 + 10log$_{10}$(1000) = 24dB. The magnitude of this phase-noise signal in comparison to the thermal noise level is shown in Figure 14.

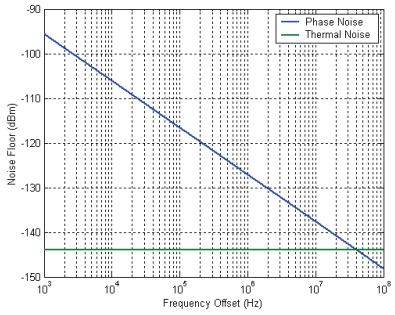

Figure 14: Comparison between phase noise and thermal noise for a radar with -20dB leakage level and 14dBm transmit power

From this graph it is clear that the radar performance is limited by the oscillator phase noise and so increasing the transmitter power will just raise the noise floor proportionally and no improvement in performance would be obtained.

4.1 Reducing Leakage Power

The only ways to increase the range performance of the homodyne configuration described are to use an oscillator that has superior phase noise characteristics or decrease the magnitude of the leakage signal.

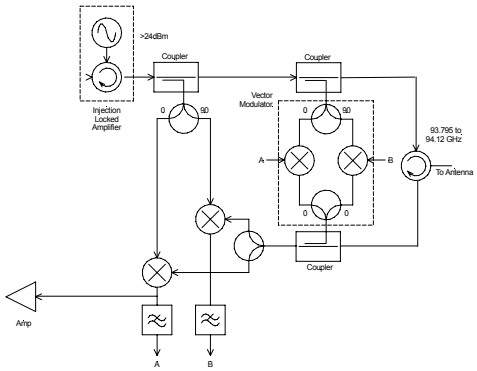

Figure 15: Adaptive leakage power cancellation technique

Reduction of the leakage signal is best achieved by using an adaptive vector modulator as shown in Figure 15. This technique has been shown to reduce the leakage power by 40dB over a wide frequency range at X-band [12], but due to manufacturing accuracy issues, similar performance is unlikely to be achieved at W-band.

The primary advantage of the adaptive cancellation technique is that it can maintain the lowest leakage irrespective of the transmitter frequency, and hence limitations to the swept bandwidth are not an issue. Additionally, if the control loop bandwidth is widened, it is also capable of cancelling close-in clutter returns that also have an adverse effect on system performance.

In the case where the transmitted bandwidth is limited, it is possible to implement a manually adjustable reflected power canceller as shown in Figure 16 [13]. Simulations show that it produces a deep null in the leakage signal with adequate cancellation over a bandwidth of 100MHz or more if the path length differences can be controlled.

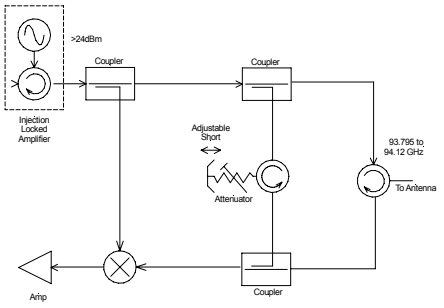

Figure 16: Adjustable vector leakage power canceller

In this configuration, as with the previous one, a small fraction of the transmitted power is coupled off and fed into a combination phase-shifter and attenuator to produce the cancellation signal whose amplitude and phase can be adjusted to match the combined reflected and leakage power from the antenna exactly.

4.2 Phase Noise around the Target

Phase noise fringes also appear around any received target, and if the target RCS is large they leak into the adjacent range bins. This results in a blurring of edges in a radar image and can even result in smaller targets being completely swamped.

In Figure 17 is shown the phase noise around a target return at a range of 100m in comparison to the raw SSB phase noise from the oscillator.

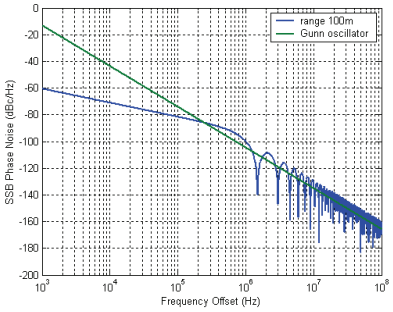

Figure 17: Phase noise around a target return at a range of 100m

To determine the noise levels in the adjacent range gates, this noise is integrated over the gate bandwidth at the appropriate offset as shown in Figure 18.

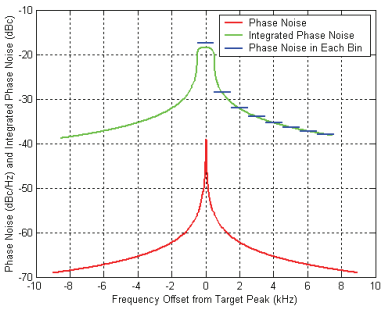

Figure 18: Phase noise and integrated phase noise in each 1kHz wide range bin around a target at a range of 100m

This figure shows the integrated phase noise power with respect to the reflected signal level in each of the range bins adjacent to the peak echo signal. In this example with a 1kHz gate bandwidth, the integrated phase noise level in the bins straddling the target is less than 29dB down on the peak signal level. This characteristic ensures that there can never be a contrast of more than 29dB across a range bin boundary irrespective the actual differences in RCS for this particular configuration. It can be shown that the contrast is further reduced as the range to the target increases.

If the RCS is large, then these phase noise skirts can swamp the returns produced by smaller targets to produce bright radial lines on images made using FMCW radars as is shown in Figure 19.

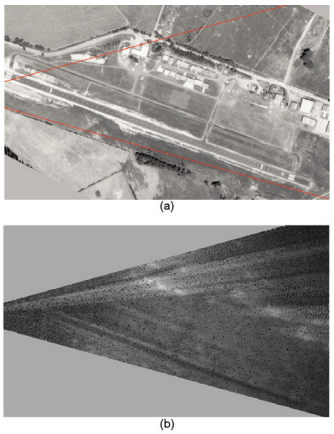

Figure 19: Airfield aerial photograph (a) and radar image (b) showing phase noise around a large target

In this case, the nearby hangars (at a range of about 400m) towards the top of the image have sufficiently large radar cross sections to lift the noise floor higher than the target echoes along that radial.

5 Conclusion

This paper shows that though the FMCW principle is straight forward, the issues that determine its performance are quite complex. Careful consideration of these aspects is required if a successful millimetre wave radar implementation is to be achieved.

6 References

[1] M. Skolnik, Radar Handbook: McGraw Hill, 1970.

[2] J. Ondria, "Novel Approaches to Wide Electronic Tuning Bandwidth in Solid State Millimeter Sources," presented at IEEE SPIE Symposium, Arlington, VA USA, 1982.

[3] L. Rabiner and B. Gold, Theory and Application of Digital Signal processing: Prentice Hall, 1975.

[4] N. Currie and C. Brown, Principles and Applications of Millimeter-Wave Radar: Artech House, 1987.

[5] G. Brooker, "Long-Range Imaging Radar for Autonomous Navigation," vol. Ph.D: University of Sydney, 2005.

[6] E. Brookner, Radar Technology: Artech House, 1982.

[7] "Hughes Millimeter-Wave Products," Microwave Products Division, 1990.

[8] F. Gardner, Phaselock Techniques, 2nd ed: John Wiley & Sons, 1979.

[9] T. Musch, I. Rolfes, and B. Schiek, "A Highly Linear Frequency Ramp Generator Based on a Fractional Divider Phase-Locked-Loop," IEEE Transactions on Instrumentation and Measurement, vol. 48, pp. 634-637, 1999.

[10] S. Maas, Microwave Mixers, 2nd ed: Artech House, 1993.

[11] J. Ondria and A. G. Cardiasmenos, "Desensitisation of Spread Spectrum Radar Systems by Far Off the Carrier Noise Generation in Millimeter Sources," presented at 2nd Military Microwaves Conference, London, England, 1980.

[12] P. B. Beasley, A. G. Stove, B. J. Reits, and B. As, "Solving the problems of Single Antenna Frequency Modulated CW Radar," presented at IEEE International Radar Conference, Arlington, VA USA, 1990.

[13] S. Kobayashi and A. Hatono, "Unwanted Signal Reflection in FMCW Radar for Measuring Slag level in BOF," presented at International Symposium on Noise and Clutter Rejection in Radars and Image Sensors, 1984.